Prioritised Objectives for Model Predictive Control of Building Heating Systems

Edward O'Dwyer[a], Luciano De Tommasi[b], Konstantinos Kouramas[b], Marcin Cychowski[b], Gordon Lightbody[a,c]

[a] *School of Engineering, University College Cork, Ireland*
[b] *United Technologies Research Centre, Cork, Ireland*
[c] *SFI MaREI Research Centre, Cork, Ireland*

Abstract

Advantages of Model Predictive Control (MPC) strategies for control of building energy systems have been widely reported. A key requirement for successful realisation of such approaches is that strategies are formulated in such a way as to be easily adapted to fit a wide range of buildings with little commissioning effort. This paper introduces an MPC-based building heating strategy, whereby the (typically competing) objectives of energy and thermal comfort are optimised in a prioritised manner. The need for balancing weights in an objective function is eliminated, simplifying the design of the strategy. The problem is further divided into supply and demand problems, separating a high order linear optimisation from a low order nonlinear optimisation. The performance of the formulation is demonstrated in a simulation platform, which is trained to replicate the thermal dynamics of a real building using data taken from the building.

Keywords: Lexicographic MPC, prioritised objectives, building energy, fault tolerance, system identification

1. Introduction

The building energy sector has been widely recognised as a significant contributor to global energy consumption and as such, the effects of human influenced climate change. Globally, as much as 20-40% of total energy usage is consumed in buildings [1], while in [2], it is stated that the services and households sector was responsible for 35% of global energy consumption in 2012. Consequently, the sector accounts for 30% of CO_2 emissions [3]. While the need for large scale improvements is clear and stricter building regulations have encouraged better insulation and more efficient equipment, it is shown in [4] that typically, modern heating systems are not used efficiently and are not adjusted to meet the needs of changing conditions.

Traditional building heating systems tend to be controlled to react to current system and environmental conditions. Due to the slow nature of the thermal dynamics associated with a building, such an approach can lead to inefficient operation and excess energy use. A promising and commonly cited alternative to current strategies is Model Predictive Control (MPC), the literature for which has been widely covered [5, 6, 7, 8]. By predicting the future state trajectory of a system and determining the optimum input sequence, MPC can account for varying heat demands in a building due to changing weather [9] and occupant usage [10, 11] before the changes occur.

Email addresses: edward.j.odwyer@umail.ucc.ie (Edward O'Dwyer), detomal@utrc.utc.com (Luciano De Tommasi), kouramk@utrc.utc.com (Konstantinos Kouramas), cychowm@utrc.utc.com (Marcin Cychowski), g.lightbody@ucc.ie (Gordon Lightbody)

While MPC has been shown to outperform typical rule-based strategies in terms of thermal and energy performance [3, 12], the potentially large number of zones in a typical building may result in a complicated objective with many, often competing, goals [13]. A strategy may often seek to optimise some comfort metric in all occupied zones for example, while using as little energy as possible. If improving the comfort within a zone requires more energy, some balance must be assigned to dictate an acceptable trade-off between energy savings and comfort satisfaction. This balance is dependent on the thermal dynamics of each individual zone [14]. Consideration of all zones in a single objective requires the appropriate selection of many tuning parameters.

In this paper a prioritised formulation is introduced which seeks to achieve improved comfort and energy performance allied to a level of scalability and flexibility which would allow it to be commissioned and reconfigured without the need for an intricate system-specific parameter selection process. A lexicographic formulation is developed to handle the competing objectives of comfort and energy. The satisfaction of comfort criteria in all zones is first established, followed by a minimisation of the energy required to achieve the optimised comfort level. Furthermore, it is shown that in the case of faults, using such a strategy allows for objectives associated with individual zones to be removed from the formulation without the need for reassigning weights in the objective.

An additional optimisation layer in the control hierarchy is then introduced to enable nonlinearities associated with the heating system to be included separately to the

high-order linear lexicographic problem. The overall formulation then consists of three layers of optimisation. The first and second are linear and quadratic programs respectively with a potentially high number of variables and constraints (related to the product of the number of zones in the building and the length of the prediction horizon). The final layer is a nonlinear optimisation problem with a lower number of variables and constraints (proportional to the prediction horizon).

To assess the performance of the strategy, a simulation platform is developed based on an RC-network analogy commonly used in building modelling. Using a validated platform in place of a real building allows for the analysis and comparison of different strategies with consistent external conditions. The parameters of the simulation model are calibrated using a metaheuristic optimisation algorithm so that the thermal dynamics of the simulation platform replicate those of a real building. This is achieved using measured data from the building. To account for unmeasured disturbances and the corrupting impact they might have on the identification process, a disturbance estimation method is used based on a spatial filtering process using Principal Component Analysis (PCA). Low-order zone models are then derived from the measured building data for use within the control formulation, once again incorporating the disturbance estimation techniques.

The prioritised MPC formulation is implemented in the simulation platform and compared in terms of energy consumption and thermal comfort with the weather compensation strategy which is currently employed for this building. It is then shown how the strategy can be adjusted to reduce energy at the expense of comfort by the end user. The adjustment is tangible in nature as it only concerns acceptable widths of zone temperature comfort bands (in $^{\circ}C$). Finally, it is shown that a fault in one zone of the system does not affect the control of the remaining zones if the fault is accounted for in the prediction models. All results are obtained in simulation.

In Section II, a prioritised-objective formulation is outlined, separating the objectives of energy and comfort. The reconfigurability of the formulation in the event of faults is also demonstrated. Section III considers the issue of incorporating nonlinear heating equipment in a strategy with a large number of variables and constraints. In Section IV, the full set of constraints and objectives for each level of the control hierarchy is derived. The performance of the strategy is assessed in Section V, using a simulation platform, developed to represent the thermodynamic properties of a real building, using measured data from the building.

2. Control

2.1. Background

The performance objectives of foremost importance to any building heating (or cooling) system control strategy could be separated into two main categories: reduction of energy consumption and satisfaction of the occupant's comfort demands [15]. The former objective is the more conceptually unambiguous, typically consisting of a cost in terms of units of energy [5, 12] or units of currency [16, 17].

The comfort objective can be somewhat more abstract. Crucially, the notion of *comfort satisfaction* in a general sense is subjective to each individual occupant. A commonly used index for quantifying comfort is the Predicted Mean Vote (PMV) which is used for predictive control purposes in [18] and [19]. Limitations associated with the use of PMV are outlined in [20] in which it is noted that in surveys of individual buildings, the actual observed mean vote often does not correspond to calculated values. Furthermore, as the PMV model is nonlinear and quite complicated, it may be more suited to model-free approaches. For many strategies [3], particularly those for which humidity control is not available (as is the case for the hydronic heating system studied here), a comfort cost based on the deviation of the zone temperature from a given set-point is used. For the remainder of this chapter, *comfort* is defined by the proximity of a zone temperature to its set-point.

In typical MPC formulations, a state-space structure is used for the optimisation model, with a constrained numerical optimisation employed to determine the future control sequence [21, 22]. The cost function at the k^{th} sample is often of the form:

$$J(k) = \sum_{i=1}^{H} \|\hat{z}(k+i) - r(k+i)\|_{\mathcal{Q}}^2 + \sum_{i=0}^{H-1} \|\Delta\hat{u}(k+i)\|_{\mathcal{R}}^2 \quad (1)$$

where $\hat{z}(k+i)$ is the output predicted for i steps in the future, $r(k+i)$ is some desired reference, and $\hat{u}(k+i)$ is the predicted input, using a H-step prediction horizon.

This objective is formulated so as to minimise the deviation between the plant and the reference, with the control increment included to introduce integral action to the formulation [21]. The reasoning behind this standard cost function does not however naturally extend to the problem of building heating systems. Building energy control typically seeks to minimise the deviation of the outputs (the zone temperatures) from a reference, while also minimising the sum of the inputs (or squared inputs) to reduce energy supplied to the building, as opposed to the sum of the input increments:

$$J(k) = \sum_{i=1}^{H} \|\hat{z}(k+i) - r(k+i)\|_{\mathcal{Q}}^2 + \sum_{i=0}^{H-1} \|\hat{u}(k+i)\|_{\mathcal{R}}^2 \quad (2)$$

Variations of this cost formulation can be seen in the building energy literature [23, 24]. By the nature of the

problem, as energy is often required to improve comfort, the twin objectives of set-point tracking and input reduction will tend to oppose each-other. The result of this will be a cost function that attempts to strike a balance between comfort and energy, the bias of which will dependent on how the function is weighted. This is a subjective problem which will vary with the preference of the user and the specifics of the models used. A strategy in which a non-trivial tuning procedure is required for each building in which the strategy is used is far from ideal.

A common strategy employed to avoid the inclusion of contradicting objectives in a single cost function is to use an economic MPC formulation where only the energy supplied is minimised [10, 25, 12]. By minimising the energy cost as opposed to the squared energy cost, this form is more intuitively appealing. Often the zone temperatures are included in the constraints rather than in the cost function through the addition of a temperature band constraint [26]. If hard comfort constraints are used, the optimisation problem may become infeasible (due to limits on the inputs). For robustness, to soften these constraints, slack variables are introduced [27] which, once again, must be included in the cost function with appropriately tuned weights.

Prediction uncertainty feasibility is accounted for in [28, 6] by the use of stochastic MPC with chance constraints. An appropriate formulation of these constraints still requires a balancing of the performance with the level of acceptable constraint violation.

In order to avoid the feasibility issues and the difficult weight tuning problem, this paper proposes a methodology by which competing objectives are minimised separately. The problem is divided into demand-side (how much energy is required in the building) and supply-side (how the energy is delivered to the building) optimisation problems. The demand-side strategy is formed as a multi-objective problem whereby the occupant comfort is taken as the primary objective to be minimised; the determination of the minimum energy required to achieve this comfort level is then taken as the secondary objective. The supply-side problem seeks to control the heating system in a way that delivers this energy with the greatest efficiency. Dividing the problem in this manner allows for a multi-layer control hierarchy (as is typically the case in larger buildings) to be taken into account more readily, without increasing the complexity of the problem.

2.2. Prioritised Objectives

For systems with a large number of controllable outputs, expressing all objectives in a single, appropriately weighted cost function can pose challenges due to the number of decision variables present. For certain systems, decomposing the problem into several objectives which are solved individually can provide a more natural framework for strategy design. A typical multi-objective formulation seeks a Pareto-optimal solution to each of the objectives, with the overall solution then being a Pareto-front, a solution set in which decreasing the cost of one objective cannot be achieved without increasing the cost of at least one other objective. Specifically, for a set of n objectives, $\boldsymbol{V}(\boldsymbol{\theta}) := [V_1(\boldsymbol{\theta}) \cdots V_n(\boldsymbol{\theta})]^T$, a Pareto optimal minimiser, $\boldsymbol{\theta}^* \in \Theta$, is one for which no point $\boldsymbol{\theta} \in \Theta$ exists that satisfies $V_i(\boldsymbol{\theta}) < V_i(\boldsymbol{\theta}^*)$ and $\boldsymbol{V}(\boldsymbol{\theta}) \leq \boldsymbol{V}(\boldsymbol{\theta}^*)$ for $i \in \{1, \cdots, n\}$, where Θ is the set of feasible solutions. An overview of multi-objective optimal control is given in [29].

In [30], a lexicographic strategy in which priorities are assigned to the objectives was outlined. Arranging the objectives in order of descending priority from $1 \ldots n$, the argument $\boldsymbol{\theta}^* \in \Theta$ is a lexicographic minimiser of the overall problem if and only if:

$$\boldsymbol{\theta}^* \in \{\boldsymbol{\theta} \in \Theta | V_j(\boldsymbol{\theta}) \leq V_j^*, j = 1, \cdots, n\} \tag{3}$$

where, for $i \in \{2, \cdots, n\}$:

$$V_1^* = \min_{\boldsymbol{\theta} \in \Theta} V_1(\boldsymbol{\theta}) \tag{4}$$

$$V_i^* = \min_{\boldsymbol{\theta} \in \Theta} \{V_i(\boldsymbol{\theta}) | V_j(\boldsymbol{\theta}) \leq V_j^*, j = 1, \cdots, i-1\} \tag{5}$$

Approaching the problem in this manner ensures that lower priority objectives are only improved if doing so does not have a detrimental effect on higher priority objectives. As a result of this ordering, weighting the objectives is not necessary. Furthermore, individual objectives can be removed or reordered without rebalancing the problem. An in-depth analysis on the fault tolerance capabilities as well as the general benefits for controller design possible by the use of a lexicographic approach can be found in [30, 31, 32].

While the advantages are clear, the problem must be formulated in a suitable framework. Crucially, the first $n-1$ objectives should not be strictly convex, as a unique solution would render lower priority objectives unnecessary.

In the application of building heating system control, the main objectives to be considered are those of minimising temperature set-point deviation in all zones of the building, while also minimising energy consumption. Achieving the former requires driving all zone temperatures, $\boldsymbol{T}_z$, as close as possible to some comfort set-point, $\boldsymbol{T}_{sp}$, over some prediction horizon H when the building is in use. The latter objective seeks to reduce the accumulated energy input to the heating system over the horizon, $\int_t^{t+H\Delta t} P_{in}(t)dt$. To accommodate these aims into a lexicographic framework, comfort satisfaction is taken as the primary objective while the energy consumption is minimised subject to the constraint that comfort is not impacted.

2.3. Cost Function Development

To ensure a generally unique solution is not obtained for the primary objective, the set-point is replaced by a temperature band $\boldsymbol{T}_{sp}^- < \boldsymbol{T}_z < \boldsymbol{T}_{sp}^+$. The deviation in

zone temperature away from this band is penalised by the introduction of slack variables $\bar{\boldsymbol{\epsilon}}$ and $\underline{\boldsymbol{\epsilon}}$. These are vectors comprised of the zone temperature deviations from the set-point in each zone over the prediction horizon. Denoting the set of optimisation variables as $\boldsymbol{\theta} = \left[\bar{\boldsymbol{\epsilon}}^T, \underline{\boldsymbol{\epsilon}}^T, \boldsymbol{P}_{in}^T\right]^T$, the primary optimisation at time k can be formed (at this point ignoring heating system constraints) as:

$$V_1^* = \min_{\boldsymbol{\theta}} \Pi_1 \boldsymbol{\theta} \tag{6}$$

$$s.t.$$

$$\bar{\boldsymbol{\epsilon}}(k+i) \geq \boldsymbol{T}_z(k+i) - \boldsymbol{T}_{sp}^+ \tag{7}$$

$$\underline{\boldsymbol{\epsilon}}(k+i) \geq \boldsymbol{T}_{sp}^- - \boldsymbol{T}_z(k+i) \tag{8}$$

$$\bar{\boldsymbol{\epsilon}}, \underline{\boldsymbol{\epsilon}} \geq 0 \tag{9}$$

$$i \in \{1, \ldots, H\}$$

For a building of N zones, the vector $\Pi_1 \in \Re^{H(2N+1)}$ is given by:

$$\Pi_1 = \begin{bmatrix} \mathbf{1}_{NH}^T & \mathbf{1}_{NH}^T & 0_{1\times H} \end{bmatrix}, \tag{10}$$

where $\mathbf{1}_{NH}$ is a column of NH ones. The linear cost is convex, but not strictly convex and so the solution is not generally unique.

The secondary objective can then be expressed as:

$$V_2^* = \min_{\boldsymbol{\theta}} \boldsymbol{\theta}^T \Pi_2 \boldsymbol{\theta} \tag{11}$$

$$s.t.$$

$$V_1(\boldsymbol{\theta}) \leq V_1^*, \tag{12}$$

where in this case:

$$\Pi_2 = \left[\begin{array}{c:c} 0_{2NH\times 2NH} & 0_{2NH\times H} \\ \hdashline 0_{H\times 2NH} & I_{H\times H} \end{array}\right] \tag{13}$$

On first inspection, the cost function does not appear to be strictly convex as Π_2 is semi-positive definite. As this is the final objective, a unique solution is desirable. Considering however that the minimum of $V_1(\boldsymbol{\theta})$ has been found in (6), the constraint given by (12) ensures that $V_1(\boldsymbol{\theta}) = V_1^*$. As this is a constant, it can be added to the cost function without affecting the solution:

$$\boldsymbol{\theta}^* = \arg\min_{\boldsymbol{\theta}} \left(\boldsymbol{\theta}^T \Pi_2 \boldsymbol{\theta} + V_1(\boldsymbol{\theta})\right) \tag{14}$$

The cost function can now be rewritten as:

$$V(\boldsymbol{\theta}) = \boldsymbol{P}_{in}^T \boldsymbol{P}_{in} + [1, \cdots, 1] \begin{bmatrix} \bar{\boldsymbol{\epsilon}} \\ \underline{\boldsymbol{\epsilon}} \end{bmatrix}, \tag{15}$$

which can be shown to be a strictly convex function as:

$$\lambda V(\boldsymbol{\theta}_1) + (1-\lambda) V(\boldsymbol{\theta}_2) > V\left(\lambda \boldsymbol{\theta}_1 + (1-\lambda)\boldsymbol{\theta}_2\right) \tag{16}$$

$$\lambda \in [0, 1]$$

2.4. Reconfiguration

The fault tolerant properties of MPC have been widely studied [33, 34, 35, 36]. A certain amount of passive fault tolerance can be exhibited without knowledge of the fault [37]; however for active fault tolerance, if knowledge of the fault is available, the constraints and objectives must be updated to reflect the post-fault operation of the system.

As previously referred to, when using a standard single cost function formulation such as (2), a large number of weighting parameters are required to balance the comfort objectives in each zone with the energy minimisation objective. Typically, these weights will be designed for a disturbance-free, fault-free scenario. In the presence of disturbances and faults however, the balance between comfort and energy can become somewhat arbitrary [30]. Even if the changes to the system are accounted for in the constraints, the cost function must be recomputed in order to obtain some desired performance [14].

The need for retuning is illustrated in the following example where the temperatures of two zones are controlled by a single input using an MPC strategy with the cost function given by (2):

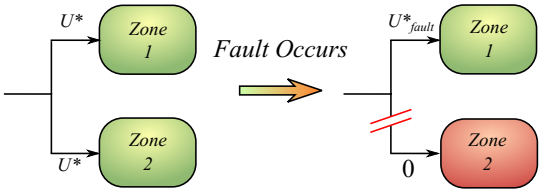

Figure 1: Controlling 2 zones - Reconfiguration in Fault Scenario

The sequence of zone temperatures ($\boldsymbol{T}_{z1}$ and $\boldsymbol{T}_{z2}$) over the prediction horizon H at time k is expressed in terms of the sequence of inputs $\boldsymbol{U}(k)$ and current zone states $\boldsymbol{x}_1(k)$ and $\boldsymbol{x}_2(k)$ as:

$$\begin{bmatrix} \boldsymbol{T}_{z1} \\ \boldsymbol{T}_{z2} \end{bmatrix} = \begin{bmatrix} \Psi_1 & 0 \\ 0 & \Psi_2 \end{bmatrix} \begin{bmatrix} \boldsymbol{x}_1(k) \\ \boldsymbol{x}_2(k) \end{bmatrix} + \begin{bmatrix} \Pi_1 \\ \Pi_2 \end{bmatrix} \boldsymbol{U}(k) \tag{17}$$

The optimal unconstrained solution of (2) for the input sequence is then [21]:

$$\boldsymbol{U}^*(k) = \left(\begin{bmatrix} \Pi_1^T & \Pi_2^T \end{bmatrix} \mathcal{Q} \begin{bmatrix} \Pi_1 \\ \Pi_2 \end{bmatrix} + \mathcal{R}\right)^{-1} \begin{bmatrix} \Pi_1^T & \Pi_2^T \end{bmatrix} \mathcal{Q} \begin{bmatrix} \boldsymbol{\xi}_1 \\ \boldsymbol{\xi}_2 \end{bmatrix}_k \tag{18}$$

where $\mathcal{Q}$ and $\mathcal{R}$ are the tuning matrices and $\boldsymbol{\xi}_1$ and $\boldsymbol{\xi}_2$ are the predicted sequence of free response set-point deviations over the prediction horizon at time k. This relationship represents the balance between energy consumption (the accumulated input) and comfort satisfaction (the set-point deviation) in each of the zones.

A scenario is now considered whereby control of the second zone is lost (a stuck valve, for example, may block the input). The best approach may be to remove the faulted zone from the optimisation problem without affecting the energy/comfort balance of the unfaulted zone.

Given knowledge of the fault, the formulation could be reconfigured to simulate the presence of the fault (and remove the faulted zone set-point deviation from the cost function) by setting $\Pi_2 = 0$. The new optimal solution of the unconstrained problem is:

$$\boldsymbol{U}^*_{fault}(k) = \left(\Pi_1^T \tilde{\mathcal{Q}} \Pi_1 + \mathcal{R}\right)^{-1} \Pi_1^T \tilde{\mathcal{Q}} \boldsymbol{\xi}_1(k), \tag{19}$$

where $\mathcal{Q} \in \Re^{H \times H}$ is given by $\tilde{\mathcal{Q}}_{i,j} = \mathcal{Q}_{i,j}$, for $i = 1, 2, ...H$ and $j = 1, 2, ...H$.

Though the set-point deviation term of the faulted zone has been eliminated from the cost, the balance between the input and the un-faulted zones set-point deviation has been altered. To achieve the same balance as the pre-faulted scenario, the tuning matrices must be recalculated. In the case of a building with a large number of zones and actuators, pre-defined weightings for all possible combinations of fault scenarios quickly becomes intractable.

Using a lexicographic approach however, as no tuning is required, the post-fault behaviour of the system is predefined [31] and a fault of this class in one zone does not propagate across the building. The primary and secondary objectives remain unchanged before and after the fault, provided the fault has been accounted for in the model (in this example, by setting $\Pi_2 = 0$).

3. Modelling

3.1. Heating System & Control Inputs

In order to incorporate the constraints associated with the thermodynamics of the building into the prioritised framework, the heating system must first be considered. In a modern office building, a hydronic heating system will typically consist of three layers. At the highest level, enough heat energy must be produced (using boilers, Combined Heat and Power units (CHPs) or heat pumps) to heat the building as a whole. The heat must then be distributed from the system header to all parts of the building at a suitable temperature. Finally, thermostatic valves allow radiators in each zone to switch off if the zone temperature exceeds a set-point. In this case, the heat is assumed to be generated using a boiler, while the temperature of the water supplied to all radiators on each floor is dictated by PI-controlled mixing valves (which combine supply water with water returning from the radiators). The zone-level thermostatic valves follow a hysteresis loop. In Fig. 2, the three layers of the heating system hierarchy are shown for a building of F floors.

Maintaining the autonomy of the lowest layer (the zone-level thermostatic valves) is desirable for robust operation [21, 14]. The MPC formulation is then focused on the mixing valves and the boiler, while the zone-level valves operate as per the hysteresis loop of the standard strategy. The inputs to the mixing valves are the set-points of the PI-controllers which control the temperature of the water flowing to the radiators on each floor, ($T_{fl_{sp}}$), while the input to the boiler is the input-power (P_{in}).

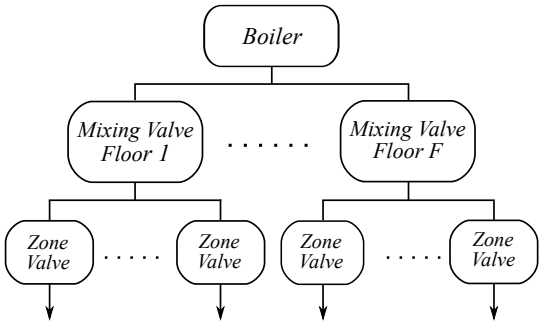

Figure 2: Three-layer heating system control hierarchy

3.2. Heat Balance

To form the constraints of the MPC strategy, the heat flow from the mixing valves to the M_i zones on the i^{th} floor are described by the following set of equations ($j \in \{1, \ldots, M_i\}$):

$$\boldsymbol{x}_{i,j}(k+1) = A_{i,j}\boldsymbol{x}_{i,j}(k) + B_{i,j}T_{fl_{sp_i}}(k) + E_{i,j}T_e(k) \tag{20}$$

$$T_{z_{i,j}}(k) = C_{i,j}\boldsymbol{x}_{i,j}(k) \tag{21}$$

$$Q_{MV_i}(k) = \sum_{j=1}^{M_i} \delta_{i,j}\left(T_{fl_{sp_i}}(k) - T_{z_{i,j}}(k)\right) \tag{22}$$

where Q_{MV_i} is the heat flow from the mixing valves to the i^{th} floor, while T_e and $T_{z_{i,j}}$ are the external and j^{th} zone temperatures respectively. Here, $\delta_{i,j}$ represents the heat transfer coefficient which is assumed to be constant. In [25] a strategy is developed to take into account the non-linearity associated with this term.

The header dynamics are described using the heat flow into the header from the boiler and the heat flow out of the header to the mixing valves on each of the F floors as:

$$T_h(k+1) = T_h(k) + \frac{1}{\beta}\left(Q_{Bo}(k) - \sum_{i=1}^{F} Q_{MV_i}(k)\right), \tag{23}$$

where Q_{Bo} is the heat output of the boiler and β is a constant representing the thermal capacity of the header. The relationship between the input power to the boiler P_{in} and the output from the boiler, where η denotes the boiler efficiency is given as:

$$P_{in}(k)\eta(k) = Q_{Bo}(k) \tag{24}$$

3.3. Boiler Efficiency

The boiler efficiency η, is often given by the manufacturers efficiency curves as a function of the power input and the return water temperature (which in this case is the header temperature). In Fig. 3 for example, the relationship between Q_{Bo} and P_{in} is shown for two different header temperatures determined using efficiency curves given for the *Viessmann Virocrossal 200* series of boiler.

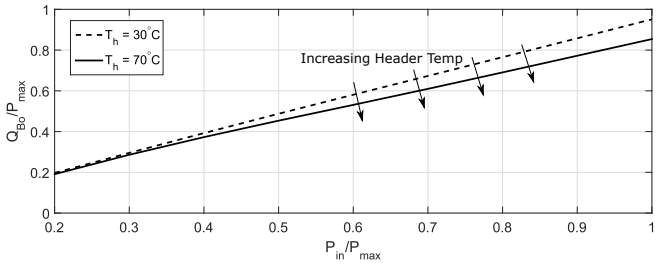

Figure 3: Boiler input and output power for different values of T_h

With this information, it is then possible to approximately fit a nonlinear efficiency surface to data-points taken from these curves that relates Q_{Bo} to T_h and the input power P_{in}:

$$Q_{Bo}(k) = f\left(T_h(k), P_{in}(k)\right) \tag{25}$$

The heating system equations must be included in the control strategy in the form of constraints. An important consideration here however, is that the relationship between the boiler input and output power is not linear (25). Furthermore, the operating region of operation for a boiler is often discontinuous. Though it may be switched off, operating the boiler at less than a specific input power may not be permissible. The operating range is then given by the discontinuous interval $P_{in}(t) \in \{0 \cup [P_{min}, P_{max}]\}$. Approaches for solving nonlinear optimisation problems have been widely studied [38, 39], however, in many cases both the objective and constraints are assumed to be not only continuous, but twice-continuously differentiable [40, 41]. Though methods for Nonlinear Mixed Integer Linear Programming (MINLP) and combinatorial programming exist [42], such problems are generally NP-hard [43], becoming prohibitively complex as the number of variables and constraints increases.

To avoid discontinuity, the variable Q_{Bo} is replaced by the continuous function Q'_{Bo}, given by:

$$Q'_{Bo}(k) = \frac{1}{2}\left(1 + \tanh\left[\rho\left(\frac{P_{in}(k) - P_{min}}{P_{max}}\right)\right]\right) Q_{Bo}(k) \tag{26}$$

Though solutions within the region $(0, P_{min})$ are now possible, the tanh function renders such solutions less desirable. The constant ρ determines the *steepness* of the tanh function. For $\rho = 10$, the efficiency surface can be represented as:

Including this relationship in the two-level optimisation framework formulated in *Section II* results in a pair of nonlinear problems that are not generally convex, with $H(2N + F)$ variables to be found where N is the total number of zones. While methods for solving such minimisation problems are available [41], quickly determining a solution in larger buildings with many zones and floors may become difficult. To avoid this here, the overall formulation is separated into a demand-side problem and a

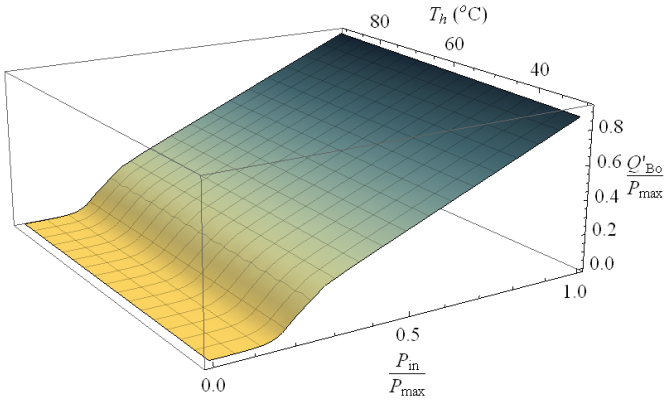

Figure 4: Boiler output as a function of boiler input & header temperature

supply-side problem, formed in such a way as to decouple the nonlinear terms of supply-side problem from the large number of variables associated with the potentially numerous zones and floors of the demand-side problem, thus allowing for the strategy to be scaled more easily. The demand-side problem uses the lexicographic approach as described, with the heat input to each floor of the building (from the header) Q_{MV_i} used in place of P_{in}. The setpoints $T_{fl_{sp_i}}$ to be sent to the mixing valves are deduced from $Q^*_{MV_i}$. The boiler is only considered in terms of the limits it puts on the available heat and so only the maximum output power Q^+_{Bo} is required. The non-linearities of (26) can then be omitted from the formulation.

Once a unique solution for the heat to be supplied to all floors of the building, $\boldsymbol{Q}^*_{MV} = \sum_1^F Q^*_{MV_i}$, has been established, it is possible to ignore all constraints associated with the zones and just determine the minimum boiler input power P_{in} needed to supply $\boldsymbol{Q}^*_{MV}$. This supply-side problem contains the nonlinear boiler dynamics, but only comprises H variables. The complete framework is shown in Fig. 5.

4. Formulation of Prioritised-Objective Control Strategy

This section outlines the full set of constraints and objectives for each layer of the hierarchy for a building of N zones and F floors.

4.1. Demand-Side

The vector of M_i predicted zone temperatures on the i^{th} floor over a horizon of length H, represented by:

$$\begin{aligned}\boldsymbol{T}_{z_i}(k) = \Big[&T_{z_{i_1}}(k+1), T_{z_{i_2}}(k+1) \cdots T_{z_{i_{M_i}}}(k+1) \cdots \\ &\cdots T_{z_{i_1}}(k+H), T_{z_{i_2}}(k+H) \cdots T_{z_{i_{M_i}}}(k+H)\Big]^T\end{aligned} \tag{27}$$

is given as:

$$\boldsymbol{T}_{z_i}(k) = \Psi_i \boldsymbol{x}_{0_i}(k) + \Phi_i \boldsymbol{T}_{fl_{sp_i}}(k) + \varphi_i \boldsymbol{T}_e(k), \tag{28}$$

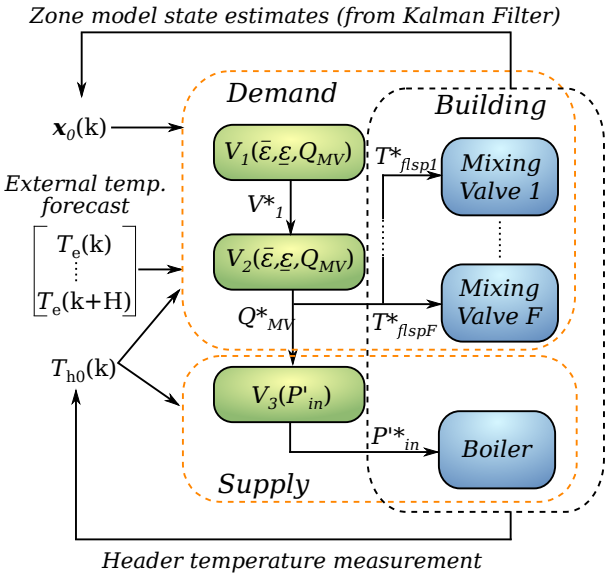

Figure 5: Three-layer control hierarchy

where, with $\bigoplus$ denoting the direct sum operation:

$$\Psi_i = \begin{bmatrix} \bigoplus_{j=1}^{M_i} C_{i,j} A_{i,j} \\ \vdots \\ \bigoplus_{j=1}^{M_i} C_{i,j} A_{i,j}^{H} \end{bmatrix}$$

$$\Phi_{i_{(j-1)M_i+q,r}} = \begin{cases} C_{i,q} A_{i,q}^{j-r} B_{i,q}, & \text{if } j-r \geq 0 \\ 0, & \text{otherwise} \end{cases}$$

$$\varphi_{i_{(j-1)M_i+q,r}} = \begin{cases} C_{i,q} A_{i,q}^{j-r} E_{i,q}, & \text{if } j-r \geq 0 \\ 0, & \text{otherwise} \end{cases}$$

$$\boldsymbol{T}_{fl_{sp_i}}(k) = \left[T_{fl_{sp_i}}(k) \cdots T_{fl_{sp_i}}(k+H-1)\right]^T$$
$$\boldsymbol{T}_e(k) = \left[T_e(k) \cdots T_e(k+H-1)\right]^T$$
$$j \in \{1, \cdots, H\}, \quad r \in \{1, \cdots, H\}, \quad q \in \{1, \cdots, M_i\}$$

Using (22) and (28), the heat supplied to the i^{th} floor over the horizon H, given by:

$$\boldsymbol{Q}_{MV_i} = \left[Q_{MV_i}(k+1) \cdots Q_{MV_i}(k+H)\right]^T, \tag{29}$$

can be expressed in terms of $\boldsymbol{T}_{fl_{sp_i}}$ as:

$$\boldsymbol{Q}_{MV_i} = (I_H \otimes \boldsymbol{\delta}_i)\left(\left(I_H \otimes \mathbf{1}_{M_i} - \Phi_i\right)\boldsymbol{T}_{fl_{sp_i}} - \boldsymbol{y}_{f_i}\right), \tag{30}$$

where $\otimes$ is the Kronecker product [44], I_H denotes a $H \times H$ identity matrix, $\boldsymbol{\delta}_i$ is a row vector of heat transfer coefficients associated with each of the zones (taken from (22)) and $\boldsymbol{y}_{f_i}$ is the free response of the zone models, given by $\boldsymbol{y}_{f_i} = \Psi_i \boldsymbol{x}_{0_i} + \varphi_i \boldsymbol{T}_e$.

Denoting for brevity:

$$\Lambda_{1_i} = (I_H \otimes \boldsymbol{\delta}_i)$$
$$\Lambda_{2_i} = \left(I_H \otimes \mathbf{1}_{M_i} - \Phi_i\right)$$
$$\Lambda_{3_i} = \left(\Lambda_{1_i}\Lambda_{2_i}\right)^{-1},$$

the constraints of (7-8) can then be written for all N zones of the building in terms of the optimisation variables $\boldsymbol{\theta} = \left[\bar{\boldsymbol{\epsilon}}^T, \underline{\boldsymbol{\epsilon}}^T, \boldsymbol{Q}_{MV_1}^T, \cdots, \boldsymbol{Q}_{MV_F}^T\right]^T$ as:

$$\left[\begin{array}{c|c} -I_{2NH} & \begin{array}{c} \bigoplus_{i=1}^{F} \Phi_i \Lambda_{3_i} \\ \hline -\bigoplus_{i=1}^{F} \Phi_i \Lambda_{3_i} \end{array} \end{array}\right] \boldsymbol{\theta} \leq \left[\begin{array}{c} \boldsymbol{T}_{sp}^{+} - \boldsymbol{y}_{f_1} - \Phi_1 \Lambda_{3_1} \Lambda_{1_1} \boldsymbol{y}_{f_1} \\ \vdots \\ \boldsymbol{T}_{sp}^{+} - \boldsymbol{y}_{f_F} - \Phi_F \Lambda_{3_F} \Lambda_{1_F} \boldsymbol{y}_{f_F} \\ \hline \boldsymbol{y}_{f_1} + \Phi_1 \Lambda_{3_1} \Lambda_{1_1} \boldsymbol{y}_{f_1} - \boldsymbol{T}_{sp}^{-} \\ \vdots \\ \boldsymbol{y}_{f_F} + \Phi_F \Lambda_{3_F} \Lambda_{1_F} \boldsymbol{y}_{f_F} - \boldsymbol{T}_{sp}^{-} \end{array}\right] \tag{31}$$

As the radiator flow temperature is controlled by mixing water from the header with return water from the radiators, the set-points, $\boldsymbol{T}_{fl_{sp_i}}$, sent to the mixing valves must be greater than or equal to the zone temperatures $\boldsymbol{T}_z$ and less than or equal to the header temperature $\boldsymbol{T}_h$. The former inequality constraint can be found in terms of $\boldsymbol{\theta}$ using (28-30) as:

$$\left[0_{NH \times 2NH} \quad -\bigoplus_{i=1}^{F} \Lambda_{2_i} \Lambda_{3_i}\right] \boldsymbol{\theta} \leq \begin{bmatrix} \Lambda_{2_1} \Lambda_{3_1} \Lambda_{1_1} \boldsymbol{y}_{f_1} - \boldsymbol{y}_{f_1} \\ \vdots \\ \Lambda_{2_F} \Lambda_{3_F} \Lambda_{1_F} \boldsymbol{y}_{f_F} - \boldsymbol{y}_{f_F} \end{bmatrix} \tag{32}$$

To ensure that enough power can be provided by the boiler when operating at maximum power Q_{Bo}^{+} to keep $\boldsymbol{T}_h$ higher than $\boldsymbol{T}_{fl_{sp}}$ and T_h^{-} (the minimum permissible header temperature) over the horizon, the following two constraints are introduced, using (23) and (30):

$$\left[\begin{array}{c|c} 0_{H(F+1) \times 2NH} & \begin{array}{c} \mathbf{1}_F \mathbf{1}_F^T \otimes \Gamma + \bigoplus_{i=1}^{F} \Lambda_{3_i} \\ \hline \mathbf{1}_F^T \otimes \Gamma \end{array} \end{array}\right] \boldsymbol{\theta} \leq \left[\begin{array}{c} T_{h0}\mathbf{1}_H + \Gamma Q_{Bo}^{+}\mathbf{1}_H - \Lambda_{3_1}\Lambda_{1_1}\boldsymbol{y}_{f_1} \\ \vdots \\ T_{h0}\mathbf{1}_H + \Gamma Q_{Bo}^{+}\mathbf{1}_H - \Lambda_{3_F}\Lambda_{1_F}\boldsymbol{y}_{f_F} \\ \hline \left(T_{h0} - T_h^{-}\right)\mathbf{1}_H + \Gamma Q_{Bo}^{+}\mathbf{1}_H \end{array}\right] \tag{33}$$

where $\Gamma \in \Re^{H \times H}$ is given by:

$$\Gamma_{i,j} = \begin{cases} \frac{1}{\beta}, & \text{for } i = j \\ 0, & \text{otherwise} \end{cases}$$

Finally, $T_{fl_{sp}}$ must be chosen to be lower than T_{fl}^{+}, the maximum permissible header temperature. Using (23), this constraint can be represented as:

$$\left[\begin{array}{c|c} 0_{FH \times 2NH} & \bigoplus_{i=1}^{F} \Lambda_{3_i} \end{array}\right] \boldsymbol{\theta} \leq \begin{bmatrix} T_h^{+}\mathbf{1}_H - \Lambda_{3_1}\Lambda_{1_1}\boldsymbol{y}_{f_1} \\ \vdots \\ T_h^{+}\mathbf{1}_H - \Lambda_{3_F}\Lambda_{1_F}\boldsymbol{y}_{f_F} \end{bmatrix} \tag{34}$$

The linear cost function and full set of constraints for the primary objective can then be expressed as:

$$V_1^* = \min_{\theta \in \Theta} \Pi_1 \boldsymbol{\theta} \tag{35}$$

$$s.t.$$

$$\Omega \boldsymbol{\theta} \leq \omega \tag{36}$$

$$\boldsymbol{\theta} \geq 0, \tag{37}$$

where the inequality in (36) is taken by stacking the set of inequalities (31-34). The matrix Ω contains the coefficients on the left-hand-side of each of these inequalities, while ω contains the terms of the right-hand-side of each. Additionally, $\Pi_1 = \begin{bmatrix} \mathbf{1}_{NH}^T & \mathbf{1}_{NH}^T & 0_{1 \times FH} \end{bmatrix}$. The secondary Quadratic Programme (QP) formulation is then:

$$V_2^* = \min_{\theta \in \Theta} \boldsymbol{\theta}^T \Pi_2 \boldsymbol{\theta} \tag{38}$$

$$s.t.$$

$$\Pi_1 \boldsymbol{\theta} \leq V_1^* \tag{39}$$

$$\Omega \boldsymbol{\theta} \leq \omega \tag{40}$$

$$\boldsymbol{\theta} \geq 0, \tag{41}$$

where

$$\Pi_2 = \begin{bmatrix} 0_{2NH \times 2NH} & 0_{2NH \times FH} \\ 0_{FH \times 2NH} & I_{FH \times FH} \end{bmatrix}$$

The flow temperature set-point $T_{fl_{sp_i}}$ to be sent to the mixing valve PI controller for the i^{th} floor can then be found using (30) from the optimal solution for $Q_{MV_i}^*$ by:

$$\boldsymbol{T}_{fl_{sp_i}} = \Lambda_{3_i} \left(\boldsymbol{Q}_{MV_i}^* + \Lambda_{1_i} \boldsymbol{y}_{f_i} \right) \tag{42}$$

$$i \in \{1, \cdots, F\}$$

4.2. Supply-Side

Having determined a unique solution for the heat energy leaving the header $\boldsymbol{Q}_{MV}^* = \sum_{i=1}^{F} \boldsymbol{Q}_{MV_i}$, the constraints associated with zones can be removed when considering the supply-side problem of minimising the boiler input power P_{in}. The variables to be considered are now P_{in}, $\boldsymbol{Q}'_{Bo}$ and $\boldsymbol{T}_h$, the latter of which can be expressed in terms of $\boldsymbol{Q}'_{Bo}$ using (23) as:

$$\boldsymbol{T}_h = T_{h0} \mathbf{1}_H + \Gamma \left(\boldsymbol{Q}'_{Bo} - \boldsymbol{Q}_{MV}^* \right) \tag{43}$$

In this problem, $\boldsymbol{T}_h$ must remain within the bounds of T_h^+ and T_h^- and above $\boldsymbol{T}_{fl_{sp}}$. The objective can be expressed as:

$$\boldsymbol{P}_{in}^* = \arg \min_{\boldsymbol{P}_{in}, \boldsymbol{Q}'_{Bo}} \sum_{k=1}^{H} P_{in}(k) \tag{44}$$

The set of linear constraints is given by:

$$\begin{bmatrix} \Gamma \\ -\Gamma \\ -(\mathbf{1}_F \otimes \Gamma) \end{bmatrix} \boldsymbol{Q}'_{Bo} \leq \begin{bmatrix} \left(T_h^+ - T_{h0}\right) \mathbf{1}_H + \Gamma \boldsymbol{Q}_{MV}^* \\ \left(T_{h0} - T_h^-\right) \mathbf{1}_H - \Gamma \boldsymbol{Q}_{MV}^* \\ T_{h0} \mathbf{1}_H - \Gamma \boldsymbol{Q}_{MV}^* - \boldsymbol{T}_{fl_{sp1}}^* \\ \vdots \\ T_{h0} \mathbf{1}_H - \Gamma \boldsymbol{Q}_{MV}^* - \boldsymbol{T}_{fl_{spF}}^* \end{bmatrix} \tag{45}$$

$$0 \leq \boldsymbol{P}_{in} \leq P_{in}^+ \mathbf{1}_H, \tag{46}$$

An additional nonlinear equality constraint is taken from (25-26) and (43):

$$\boldsymbol{Q}'_{Bo} = f(\boldsymbol{P}_{in}, T_{h0}, \boldsymbol{Q}_{MV}^*) \tag{47}$$

5. Case Study

To assess the performance and usability of the control strategy described in this paper, the implementation of the formulation in a real building, the Nimbus Centre, is considered. This is a two-floor office building located at Cork Institute of Technology which uses a hydronic heating system, such as that described in Section 3.1, to supply heat to 25 zones.

Two separate modelling strategies are outlined in Section 5.1 and Section 5.2 respectively. In the former strategy, the objective is to derive a complex high-order model of the entire building and heating system, to be used as a simulation platform. The simulation platform can then be used to represent the real building for the purpose of experimental analysis. In the second strategy on the other hand, decentralised low-order models, associated with each zone of the building, are developed to be used within the MPC strategy. In these models, long-term prediction accuracy is less important than computational simplicity. A more comprehensive analysis of the two approaches is carried out in [45].

5.1. Development of Simulation Platform

An important aspect in the development of an MPC strategy for building energy control is the availability of an appropriate simulation platform. As highlighted in [46], comparing the performance of strategies in a real building poses difficulties, primarily the ever-changing external conditions affecting the plant. A simulation platform can provide a more justifiable and consistent comparison, provided the dynamics of the platform are similar to those of a building.

Often, to obtain high-order simulations of the thermal dynamics of a building, an RC-network analogy is used [28], [47]. Walls, rooms/airspaces and windows are represented as resistances and capacitances, while temperatures and heat-flows are viewed as voltages and currents respectively. The parameters and arrangement of the components in the network are chosen to fit the materials and dimensions of the building being simulated. Using this

type of configuration allows for the building to be modelled by a set of first-order linear equations.

Such an approach is taken here with the initial network parameters taken from building properties associated with the Nimbus Centre. The RC-network used to replicate the thermal dynamics of the building consists of a 3R-2C structure for the walls, floors and ceilings, with single capacitances and single resistances used for rooms and windows respectively. The resulting state-space model is the comprised of over 800 components, 341 states, 25 outputs, 25 controlled inputs (heating system radiators) and input disturbances including external temperature, solar gains and internal gains (occupancy and equipment). The RC-network and heating system are modelled using Simulink.

5.1.1. Training of the Network

In [45], a strategy is developed in which the parameters of the physics-based RC-network are adjusted to better represent the dynamics of the building using measured data. The outlined strategy was implemented here to obtain a model of the thermodynamics of the Nimbus Centre.

Due to the large number of network parameters and the low level of possible excitation inputs, the problem is overparameterised. Taking this into consideration, as well as a desire to maintain physically realistic limits on the component values, metaheuristic search algorithms were considered to be most suitable for the training process. Using measurements of the heat supplied to the building by the heating system as well as temperature measurements for both the internal zones and the external environment, a Quantum-behaved Particle Swarm Optimisation algorithm (Q-PSO, as developed in [48]) was used to adjust the network parameters to reduce the squared output-error of the model over a period of 10 days.

5.1.2. Incorporating Disturbances

As reported in [49], model uncertainty can have a large negative impact on predictive control strategies for building energy systems. Unmeasured disturbances can corrupt any models obtained from data. Considering the inherent complexity of a building's thermodynamics as well as the relatively small range of possible excitation inputs, separating the portion of output-error due to model inaccuracy from that due to unmeasured disturbance can pose a significant challenge. Factors such as solar gain, occupancy, wind and equipment gains will typically not be measured with great accuracy, yet have too large of an impact to be ignored. In [45], an iterative technique is introduced to simultaneously estimate model parameters and unmeasured disturbances from spatio-temporally filtered input and output data using Kalman filtering and PCA, a statistical procedure used to reduce the dimensionality of a data-set of several interrelated variables [50].

In a typical building, many zones will often be affected by the same disturbance sources. Zones that are likely to be affected by similar disturbances can be grouped together (external conditions such as wind and solar gain should have a corresponding, though differently scaled, impact on geographically similar zones). Using the physics based network, disturbances were first estimated by an augmented Kalman filtering process. As the model was initially assumed to be incorrect, these disturbance estimates were considered to be a result of both model error and unmeasured disturbance. By accentuating the common unmeasured disturbance portion of the estimate, while suppressing the portion due to model error, a PCA-based spatial filtering process was used to determine a new set of less-biased disturbance estimates.

The new disturbance estimates from each group were reformed and incorporated into the Q-PSO algorithm as an additional set of inputs. A new set of model parameters were then identified and the disturbance-estimation/model-identification process was repeated. By iteratively updating the model in this manner, a simulation platform was obtained which could more accurately represent the complex dynamics of the Nimbus Centre. The strategy is illustrated in Fig. 6.

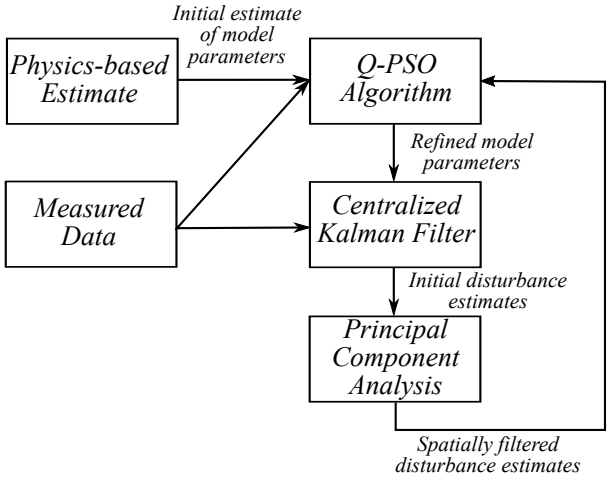

Figure 6: Simulation model identification and disturbance estimation process

The accuracy of the resulting simulation model can be seen in Fig. 7 and Fig. 8, in which the measured outputs from two zones of the building are compared to outputs obtained from the original RC-network and those obtained from the adjusted network, using an 8 day period of unseen data.

5.2. Development of Second-Order Control Models

For computation of the numerical optimisation problems (at the heart of standard MPC strategies [21], [22]), low-order, linear models are preferable. Accuracy over the prediction horizon is still paramount however - the use of inaccurate models will render any discussion of optimality meaningless. As the high-order RC-network used for simulation is unsuitable, different approaches have been taken in the literature to obtain more appropriate models. If a high-order model is available, model reduction techniques can be employed to obtain low-order zone model

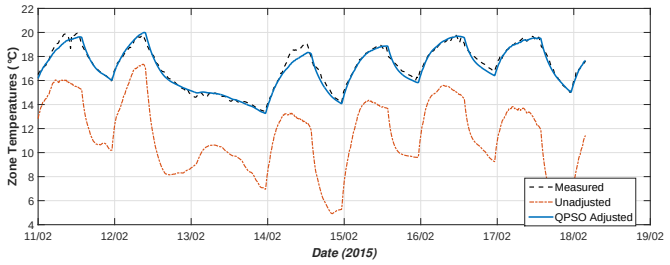

Figure 7: Q-PSO adjusted vs. original RC network comparison with real data - Ground Floor Meeting Room

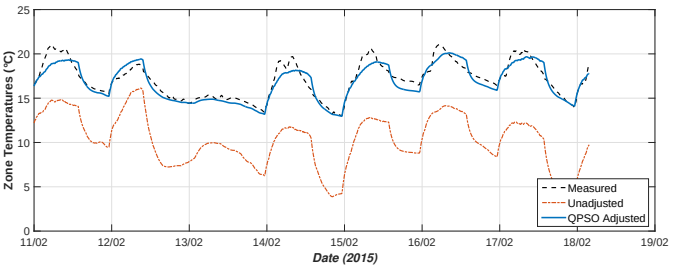

Figure 8: Q-PSO adjusted vs. original RC network comparison with real data - Ground Floor Corridor

approximations. Here, the RC-network developed in the previous section is intended to be used as a substitute for the real building. As would be the case for the real building, the internal structure of the network is considered to be unknown. Model reduction techniques must then be discounted. A review of some of the different methodologies used can be found in [51].

A sensible starting point is to consider the building as a set of zones (decentralised or distributed) [52, 24], due to the physical divide between rooms. Decomposing the large RC-network in this way can greatly simplify matters. Data-driven techniques, both black-box [26] and grey-box [53] are often used. As a detailed knowledge of materials and dimensions is not required, such approaches may be advantageous.

Using system identification and disturbance estimation techniques, individual second-order zone models were derived here using black-box methods with input and output data from each zone. A brief overview of the methodology used is provided here, while a full description can be found in [45].

The models were assigned an ARMAX (Autoregressive-moving-average model with exogenous input) structure and identified using Prediction-Error Identification Methods (PEM) before being transformed to a state-space format. The PEM algorithm sought to minimise squared output-error of each of the models. As the zone models were to fit into the strategy outlined in Section III and Section IV, the inputs used were the temperatures of water flowing to the zone radiators from the mixing valves on each floor. The outputs were the measured zone temperatures. The external temperature was also used as an additional input (a forecast of which was assumed to be available).

To better replicate the data that would be obtained from the real building using the simulation platform, disturbances representing solar gains, occupancy gains and equipment gains were generated using standard solar models and occupancy schedules. These disturbances (measurements for which were assumed to be unavailable) were applied to the platform. As for the simulation model training process, these unmeasured disturbances can have a large impact on the accuracy of the derived zone models. The spatio-temporal filtering process outlined in the previous section was used to obtain estimates for these disturbances. As the disturbances are predominantly heat based, it was assumed that they affected the model states with the same dynamics as the radiator heat inputs. In place of the centralised Kalman filter used to derive the disturbance estimates of the high-order simulation model however, a separate decentralised Kalman filter was used to determine the initial estimates for each individual zone.

These disturbance estimates were passed through the grouping and PCA spatial-filtering process, to produce a new set of estimates, which were then included as additional inputs to the zone models in the PEM algorithm. After several iterations of this process, a final set of refined second-order models was obtained. These models were then used in the MPC formulation. The identification process is shown in Fig. 9.

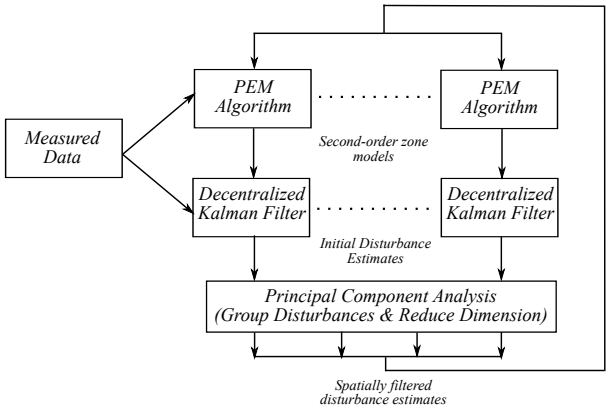

Figure 9: Zone model identification and disturbance estimation process

5.3. Performance of Prioritised Objective Strategy

Using the derived simulation platform, the performance of the prioritised-objective strategy was compared to that of the standard weather-compensation currently used in the Nimbus Centre. The zone models derived in the previous section were used in the optimisation formulations to determine the boiler input power P_{in} and the flow temperature set-points $T_{fl_{sp}}$ sent to the mixing valves. Simulations were conducted for periods representing 10 days in February and 10 days in April of 2015, using external temperature measurements taken at the Nimbus Cen-

tre. These periods were chosen as heating was required for both while the former period was significantly colder than the latter. These external temperatures are shown in Fig. 10. Unmeasured disturbances were also generated and included in the platform to represent typical solar gain, internal occupancy and equipment gain profiles for all simulations.

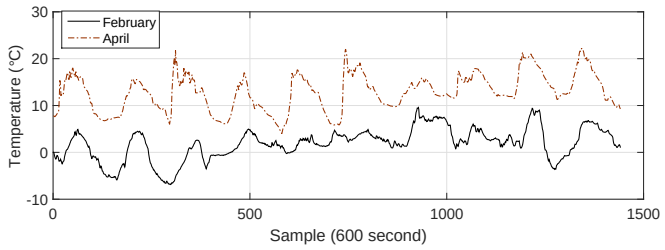

Figure 10: External temperature for February and April simulation periods

For each period, a baseline scenario was simulated using the weather compensation strategy as implemented in the real building. The flow temperature set-point was determined based on the current output temperature by the relationship: $T_{fl_{sp}}(k) = 80 - 2.5T_e(k)$. In this way, as the external temperature increases, less heat is likely to be lost by the building and as such, a lower radiator temperature can suffice. The boiler followed a hysteresis loop, switching on and off in such a way as to drive the header temperature to a band around a weather-compensated set-point.

Using the outlined MPC formulation, different scenarios were simulated for both periods, with different acceptable comfort thresholds around the $20°C$ set-point for each ($\pm 1°C$, $\pm 2°C$, $\pm 3°C$ and $\pm 4°C$ respectively). This was to illustrate how a user can save energy by selecting an appropriate level of acceptable temperature set-point deviation. With a tighter band, less deviation from the set-point (and thus, greater comfort) can be achieved, though this is likely to be at the expense of additional energy consumption.

For each of the MPC scenarios, a sample time of 600 seconds was used with a prediction horizon of 10 samples. These were chosen to reflect the time-scales at which the best zone model prediction accuracy was obtained, while also taking into account the additional complexity of longer horizons. The primary optimisation problem was solved using the *linprog* function in Matlab, the secondary was solved using the *quadprog* function, while the supply optimisation problem was solved using the Interior Point Optimiser (IPOPT) algorithm [41]. In all strategies, on/off valves in each zone were operated to follow a hysteresis loop, blocking flow to the radiator if the zone temperature exceeded a threshold of $1°C$ above a set-point (T_{sp}) of $20°C$.

To quantify the level of comfort achieved for each scenario, the accumulated deviation from the set-point is measured in each zone of the building. Summing these together, the overall building comfort can then be given in

February Scenarios

	Energy Consumption (kWh)	Set-point Deviation ($°C.hr$)
Weather Compensation	5396	1201
MPC ($20 \pm 1°C$)	4961	1105
MPC ($20 \pm 2°C$)	4854	1294
MPC ($20 \pm 3°C$)	4571	1705
MPC ($20 \pm 4°C$)	4184	2358

Table 1: Energy consumption and accumulated set-point deviation across building simulated using weather compensation and MPC strategies (February scenarios)

April Scenarios

	Energy Consumption (kWh)	Set-point Deviation ($°C.hr$)
Weather Compensation	2486	1126
MPC ($20 \pm 1°C$)	2440	831
MPC ($20 \pm 2°C$)	2293	1155
MPC ($20 \pm 3°C$)	2003	1790
MPC ($20 \pm 4°C$)	1675	2539

Table 2: Energy consumption and accumulated set-point deviation across building simulated using weather compensation and MPC strategies (April scenarios)

units of $°C.hr$, whereby $1°C.hr$ corresponds to a deviation in air temperature from the comfort set-point of $1°C$ for one hour. The energy consumptions is measured in kWh. These energy and comfort metrics are summarised for the February and April scenarios in Table 1 and Table 2 respectively.

In both periods, the MPC strategies required less energy than the weather compensation strategy, while in the case of the MPC ($20 \pm 1°C$) scenario, an improvement in comfort was also observed. The combination of energy reduction and comfort improvement illustrates the ability of the MPC formulation to more efficiently deliver heat from the boiler to the zones. The results also indicate that more energy can be saved by increasing the acceptable level of comfort in the MPC strategy. As expected, this energy saving comes at the cost of comfort.

5.4. Load Flexibility

In the simulated example shown, the use of the outlined MPC formulation allowed for an improved efficiency to be achieved when compared to standard approach. It should be noted that such an improvement is not uncommon when using MPC, with many examples in literature highlighting the benefits of an optimal control strategy for the application of building energy (a review can be found in [3]). The more significant outcome is that a more efficient performance was achievable without the need for a large-scale tuning parameter selection process, the solution to which may seem arbitrary. In this strategy, a user can explicitly

ascribe an acceptable level of discomfort to the strategy by selecting an allowed level of set-point deviation. The strategy will then attempt to satisfy this comfort requirement with as little energy as possible. This is a tangible means of adjustment, as it only concerns room temperatures (in $^{\circ}C$).

While increasing the set-point band will have the effect of reducing energy consumption, the exact relationship (knowing how much energy will be saved by increasing the band by $1^{\circ}C$ for example) will be dependent on measured and unmeasured disturbances. The potential to make energy savings by adjusting the set-point band is clear however. To illustrate this, the test scenario of the previous example was repeated using the same MPC formulation, but with different set-point bands.

In Fig. 11, the energy consumption measured for the April scenarios is plotted for comfort bands of $0.5^{\circ}C$, $1^{\circ}C$, $2^{\circ}C$, $3^{\circ}C$ and $4^{\circ}C$. It can be seen for example, that over the 10 day period, a further saving of $437kWh$ (or 18%) would be achieved if the acceptable temperature deviation was increased from $1^{\circ}C$ to $3^{\circ}C$. The internal temperatures that would result for each setting are shown for the first-floor administration office in Fig. 12.

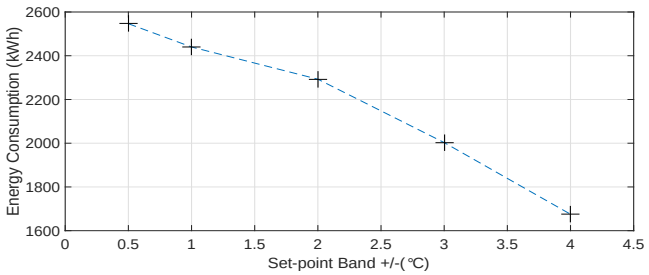

Figure 11: Energy consumption change as acceptable comfort range is increased using prioritised model predictive control strategy

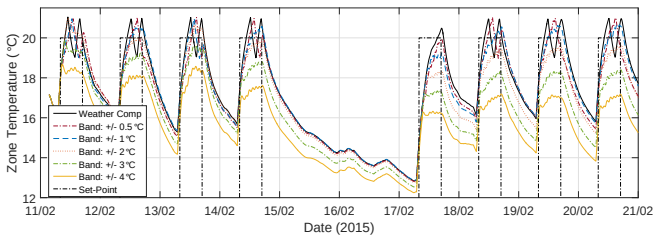

Figure 12: Simulated zone temperature obtained using weather compensation and prioritised MPC for 10 day period (first-floor administration office)

To assist in the set-point selection, the predicted load profile can also be observed. Using the full prediction horizon of the optimisation problem, a projection of the energy use can be obtained for a given period of time. By projecting the load profile for different levels of acceptable set-point deviation, an estimate can be made of the possible energy savings.

An example is shown in Fig. 13, in which a one day projection of cumulative energy use is shown for different comfort band settings, again using the February scenarios. Each of the projections was obtained by increasing the prediction horizon of the control problem to 12 hours and observing the full sequence of predicted inputs, calculated at the first time-step.

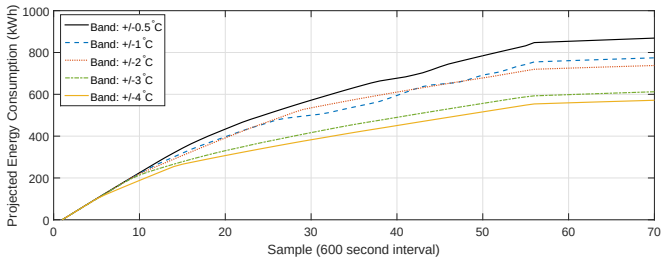

Figure 13: Projected energy consumption over period of twelve hours as acceptable comfort range is increased

In this example, it can be seen that a 21% energy reduction was predicted for the period by increasing the acceptable temperature deviation from $1^{\circ}C$ to $3^{\circ}C$. Furthermore, little advantage in terms of energy consumption was predicted to be achievable by increasing the comfort band from $1^{\circ}C$ to $2^{\circ}C$. This results from the fact that when using a wider comfort band, both over-heating and under-heating in the zones may be increased - the former acts to increase the energy consumption, while the latter acts to reduce it. A direct relationship between energy use and comfort satisfaction cannot then be assumed.

The validity of the projected energy use is dependent on the accuracy of the zone models used. As the models are selected to provide accuracy over a shorter prediction horizon, it is likely that the true daily energy use will deviate from the projected value. Additionally, disturbances will affect the true values if no disturbance prediction is available. Nonetheless, the comparison between the different set-points can be instructive when selecting an appropriate set-point band.

5.5. Reconfiguration

To illustrate the reconfigurability issues highlighted in *Section II-D*, a scenario was simulated whereby the radiator valve of the ground floor corridor was stuck in the closed position and so control to the zone was lost. Knowledge of the fault was incorporated into the prediction models by setting the gain of the input to the faulted zone to zero.

To view a more standard MPC type approach, the lexicographic formulation of the demand side problem was replaced by the single quadratic cost function as in (2). The weighting matrices $\mathcal{Q}$ and $\mathcal{R}$ were chosen to provide a similar level of comfort satisfaction to the prioritised approach used above (in this case, the energy and comfort performance of the unfaulted system is not significant, only the change in performance observed when a fault occurs).

The operation of the control strategy was simulated with and without the presence of the fault for the same February period. In Fig. 14, the simulated output of the ground floor meeting room can be seen for both scenarios. This room should be unaffected by the fault, but as can be seen (and as shown in Section 2.4), updating the constraints of the problem without recomputing the weighting matrices can impact the performance in unfaulted zones.

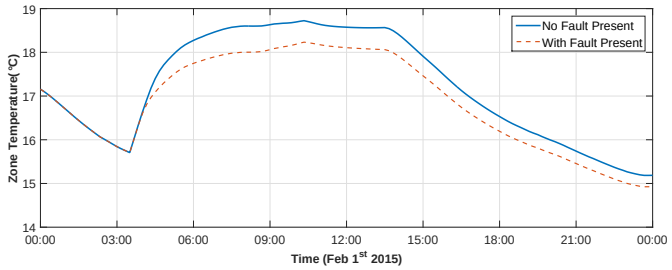

Figure 14: Simulated temperature measurement of ground floor meeting room with and without the presence of a zone level fault in corridor - Standard quadratic MPC approach

In Fig. 15, the output of the same zone is shown for the faulted and unfaulted scenarios, this time using the prioritised approach outlined in this paper. If the fault is accounted for in the constraints, no adjustment of the cost function is required. Though the solution may be different (as the system is different), the comfort and energy objectives of the unfaulted zones remains the same.

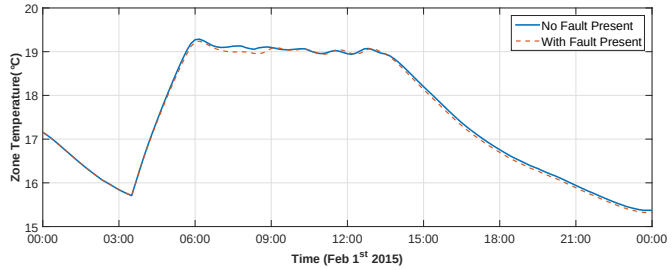

Figure 15: Simulated temperature measurement of ground floor meeting room with and without the presence of a zone level fault in corridor - Prioritised MPC approach

6. Conclusion

In this paper, a method for controlling a building's heating system was developed based on a prioritised-objective model predictive control strategy. The strategy was designed to not require an intensive tuning procedure while incorporating a large number of zones with a heating system containing nonlinear dynamics by separating the full optimisation problem into appropriate sub-problems and solving in a prioritised manner.

The issue of balancing the competing objectives of energy consumption minimisation and occupant comfort satisfaction was first addressed. A lexicographic approach was outlined whereby an acceptable temperature band for comfort satisfaction is defined for all zones. A linear optimisation determines the minimum cumulative deviation outside this band over a prediction horizon. The solution to this is used as a constraint in a second, quadratic, optimisation problem, which seeks to determine the minimum energy required to achieve this level of comfort. The cost functions of the optimisation problems do not require tuning parameters. Furthermore, it was shown that the objectives do not require reconfiguration if zones are to be removed from the strategy in fault scenarios.

In large systems with many controlled inputs and outputs (such as buildings), in addition to the issue of applying appropriate weights to large number of objectives, the complexity of the optimisation problems must be carefully considered. In the presence of discontinuities and nonlinearities associated with a heating system, an excessive level of complexity can result. In this paper a methodology was introduced whereby the full optimisation problem is further broken up into demand and supply problems. The demand problem consists of a large number of linear constraints (and variables), solved using the lexicographic approach previously outlined, while the supply problem consists of a low number of nonlinear constraints.

The strategy was tested and compared to a more standard weather compensation approach using a simulation platform designed to represent a real building. Using measured data, a model was trained to simulate the thermal dynamics of the building using a particle swarm optimisation algorithm in tandem with a principal component-based disturbance estimation strategy. Decentralised zone models are developed using prediction-error estimation methods (once again incorporating disturbance estimation) for use within the MPC strategy. The performance of the prioritised MPC approach compared favourably to weather compensation in terms of energy consumption and set-point deviation. A further analysis demonstrates the flexibility of the approach, which can be adjusted in a tangible manner, by changing the set-point band.

The robust qualities of the formulation are highlighted by simulating a system fault. It was shown that, when using a standard single objective formulation, a fault in one zone can propagate to un-faulted zones even if it has been accounted for in the prediction models, unless the weighting matrices are recomputed. The prioritised formulation outlined in this paper does not have this recomputation requirement.

7. Acknowledgements

This research was co-funded by the Irish Research Council (IRC) and United Technologies Research Center Ireland (UTRCI).

References

[1] L. Pérez-Lombard, J. Ortiz, C. Pout, A review on buildings energy consumption information, Energy and Buildings 40 (3) (2008) 394–398.

[2] IEA, Key World Energy Statistics 2014, Tech. rep. (2014).

[3] P. H. Shaikh, N. B. M. Nor, P. Nallagownden, I. Elamvazuthi, T. Ibrahim, A review on optimized control systems for building energy and comfort management of smart sustainable buildings, Renewable and Sustainable Energy Reviews 34 (2014) 409–429.

[4] L. Peeters, J. Van der Veken, H. Hens, L. Helsen, W. D'haeseleer, Control of heating systems in residential buildings: Current practice, Energy and Buildings 40 (2008) 1446–1455.

[5] Z. Liao, A. Dexter, An Inferential Model-Based Predictive Control Scheme for Optimizing the Operation of Boilers in Building Space-Heating Systems, IEEE Transactions on Control Systems Technology 18 (5) (2010) 1092–1102.

[6] F. Oldewurtel, C. N. Jones, A. Parisio, M. Morari, Stochastic Model Predictive Control for Building Climate Control, IEEE Transactions on Control Systems Technology 22 (3) (2014) 1198–1205.

[7] E. O'Dwyer, M. Cychowski, K. Kouramas, G. Lightbody, A hierarchical Model-based Predictive Control strategy for building heating Systems, in: 25th IET Irish Signals & Systems Conference 2014, Limerick, 2014, pp. 298–303.

[8] Y. Ma, F. Borrelli, B. Hencey, B. Coffey, S. Bengea, P. Haves, Model Predictive Control for the Operation of Building Cooling Systems, IEEE Transactions on Control Systems Technology 20 (3) (2012) 796–803.

[9] D. Lazos, A. B. Sproul, M. Kay, Optimisation of energy management in commercial buildings with weather forecasting inputs: A review, Renewable and Sustainable Energy Reviews 39 (2014) 587–603.

[10] F. Oldewurtel, D. Sturzenegger, M. Morari, Importance of occupancy information for building climate control, Applied Energy 101 (2013) 521–532.

[11] L. Klein, J. Y. Kwak, G. Kavulya, F. Jazizadeh, B. Becerik-Gerber, P. Varakantham, M. Tambe, Coordinating occupant behavior for building energy and comfort management using multi-agent systems, Automation in Construction 22 (2012) 525–536.

[12] D. Sturzenegger, D. Gyalistras, M. Morari, R. S. Smith, Model Predictive Climate Control of a Swiss Office Building : Implementation , Results , and Cost Benefit Analysis, IEEE Transactions on Control Systems Technology (2015) 1–12.

[13] R. Yang, L. Wang, Multi-objective optimization for decision-making of energy and comfort management in building automation and control, Sustainable Cities and Society 2 (1) (2012) 1–7.

[14] E. O'Dwyer, M. Cychowski, K. Kouramas, L. D. Tommasi, G. Lightbody, Scalable , Reconfigurable Model Predictive Control for Building Heating Systems, in: European Control Conference 2015 (ECC), 2015, pp. 2253–2258.

[15] M. Castilla, J. Álvarez, M. Berenguel, F. Rodríguez, J. Guzmán, M. Pérez, A comparison of thermal comfort predictive control strategies, Energy and Buildings 43 (10) (2011) 2737–2746.

[16] F. Oldewurtel, A. Ulbig, A. Parisio, G. Andersson, M. Morari, Reducing peak electricity demand in building climate control using real-time pricing and model predictive control, 49th IEEE Conference on Decision and Control (CDC) (2010) 1927–1932.

[17] J. Ma, J. Qin, T. Salsbury, P. Xu, Demand reduction in building energy systems based on economic model predictive control, Chemical Engineering Science 67 (1) (2012) 92–100.

[18] P. M. Ferreira, a. E. Ruano, S. Silva, E. Z. E. Conceição, Neural networks based predictive control for thermal comfort and energy savings in public buildings, Energy and Buildings 55 (2012) 238–251.

[19] R. Z. Freire, G. H. C. Oliveira, N. Mendes, Predictive controllers for thermal comfort optimization and energy savings, Energy and Buildings 40 (7) (2008) 1353–1365.

[20] M. A. Humphreys, J. Fergus Nicol, The validity of ISO-PMV for predicting comfort votes in every-day thermal environments, Energy and Buildings 34 (6) (2002) 667–684.

[21] J. Maciejowski, Predictive Control: With Constraints, Prentice-Hall, UK, 2002.

[22] E. Camacho, C. Alba, Model predictive control, 2nd Edition, Springer-Verlag, London, 2007.

[23] V. Chandan, A. Alleyne, Optimal partitioning for the decentralized thermal control of buildings, IEEE Transactions on Control Systems Technology 21 (5) (2013) 1756–1770.

[24] V. Chandan, A. G. Alleyne, Decentralized predictive thermal control for buildings, Journal of Process Control 24 (6) (2014) 820–835.

[25] I. Hazyuk, C. Ghiaus, D. Penhouet, Optimal temperature control of intermittently heated buildings using Model Predictive Control: Part II - Control algorithm, Building and Environment 51 (2012) 388–394.

[26] J. Široký, F. Oldewurtel, J. Cigler, S. Prívara, Experimental analysis of model predictive control for an energy efficient building heating system, Applied Energy 88 (9) (2011) 3079–3087.

[27] J. Cigler, S. Privara, Subspace identification and model predictive control for buildings, 2010 11th International Conference on Control Automation Robotics & Vision (December) (2010) 750–755.

[28] F. Oldewurtel, A. Parisio, C. N. Jones, D. Gyalistras, M. Gwerder, V. Stauch, B. Lehmann, M. Morari, Use of model predictive control and weather forecasts for energy efficient building climate control, Energy and Buildings 45 (2012) 15–27.

[29] A. Gambier, E. Badreddin, Multi-Objective Optimal Control: An Overview, in: IEEE International Conference on Control Applications, no. October, 2007, pp. 170–175.

[30] E. Kerrigan, J. Maciejowski, Designing model predictive controllers with prioritised constraints and objectives, IEEE International Symposium on Computer Aided Control System Design (2002) 33–38.

[31] T. Miksch, A. Gambier, Fault-tolerant control by using lexicographic multi-objective optimization, 8th Asian Control Conference (ASCC) (2011) 1078–1083.

[32] A. Gambier, MPC and PID control based on multi-objective optimization, American Control Conference, 2008 (26) (2008) 4727–4732.

[33] J. Maciejowski, X. Yang, Fault tolerant control using Gaussian processes and model predictive control, in: Conference on Control and Fault-Tolerant Systems (SysTol), 2013, pp. 1–12.

[34] E. Camacho, T. Alamo, D. de la Pena, Fault-tolerant model predictive control, Emerging Technologies and Factory Automation (ETFA).

[35] J. Boskovic, R. Mehra, Fault accommodation using model predictive methods, Proceedings of the 2002 American Control Conference (IEEE Cat. No.CH37301) 6 (2002) 4–9.

[36] Y. Zhang, J. Jiang, Bibliographical review on reconfigurable fault-tolerant control systems, Annual Reviews in Control 32 (2) (2008) 229–252.

[37] J. Maciejowski, Fault-tolerant aspects of MPC, Control: Techniques and Applications-Day 2 (1) (1999) 1–4.

[38] C. a. Floudas, Nonlinear and Mixed-Integer Optimization, Handbook of Applied Optimization (1995) 462.

[39] J. Nocedal, S. J. Wright, Numerical Optimization, Vol. 43, 1999.

[40] A. Forsgren, P. Gill, M. Wright, Interior methods for nonlinear optimization, SIAM review 44 (4) (2002) 525–597.

[41] A. Wächter, L. Biegler, On the implementation of an interior-point filter line-search algorithm for large-scale nonlinear programming, Mathematical programming 106 (1) (2006) 25–57.

[42] L. A. Wolsey, Integer Programming, Vol. 98, John Wiley & Sons, Inc., New York, 1998.

[43] C. D'Ambrosio, A. Lodi, Mixed integer nonlinear programming tools: an updated practical overview, Annals of Operations Research 204 (1) (2013) 301–320.

[44] A. J. Laub, Matrix Analysis for Scientists and Engineers, illustrate Edition, SIAM, 2005.

[45] E. O'Dwyer, L. De Tommasi, K. Kouramas, M. Cychowski,

G. Lightbody, Modelling and disturbance estimation for model predictive control in building heating systems, Energy and Buildings 130 (2016) 532–545.
[46] I. Hazyuk, C. Ghiaus, D. Penhouet, Optimal temperature control of intermittently heated buildings using Model Predictive Control: Part I - Building modeling, Building and Environment 51 (2012) 379–387.
[47] Y. Ma, A. Kelman, A. Daly, F. Borelli, Predictive control for energy efficient buildings with thermal storage, IEEE Control Systems Magazine 32 (February) (2012) 44–64.
[48] J. Sun, W. Xu, B. Feng, A global search strategy of quantum-behaved particle swarm optimization, IEEE Conference on Cybernetics and Intelligent Systems, 2004. 1 (2004) 1–3.
[49] M. Maasoumy, M. Razmara, M. Shahbakhti, a. S. Vincentelli, Handling model uncertainty in model predictive control for energy efficient buildings, Energy and Buildings 77 (2014) 377–392.
[50] I.T. Jolliffe, Principal component analysis, 2nd Edition, Vol. 2, Springer, New York, 2002.
[51] X. Li, J. Wen, Review of building energy modeling for control and operation, Renewable and Sustainable Energy Reviews 37 (2014) 517–537.
[52] C. Agbi, B. Krogh, Decentralized identification of building models, 2014 American Control Conference (2014) 1070–1075.
[53] T. Berthou, P. Stabat, R. Salvazet, D. Marchio, Development and validation of a gray box model to predict thermal behavior of occupied office buildings, Energy and Buildings 74 (2014) 91–100.